Title

Spatiotemporal reconstruction of the origin and assembly of smooth muscles in the intestinal villus

Authors

Bhargav D. Sanketi[1,†], Madhav Mantri[2,†], Mohammad A. Tavallaei[1], Shing Hu[1], Michael F. Z. Wang[2], Iwijn De Vlaminck[2,#,*], Natasza A. Kurpios[1,#,*]

Affiliations

[1] Department of Molecular Medicine, College of Veterinary Medicine, Cornell University; Ithaca, NY 14853, USA

[2] Department of Biomedical Engineering, Cornell University; Ithaca, NY 14850, USA

[†,#] These authors contributed equally

[*] Correspondence: natasza.kurpios@cornell.edu (NAK), id93@cornell.edu (IDV)

Abstract

Intestinal smooth muscles are the workhorse of the digestive system. Inside the millions of finger-like intestinal projections called villi, strands of smooth muscle cells contract to propel absorbed dietary fats through the adjacent lymphatic vessel, called the lacteal, sending fats into blood circulation for energy production. Despite this vital function, how villus smooth muscles form, how they assemble alongside lacteals, and how they repair throughout life remain unknown. Here we combine single-cell RNA sequencing of the mouse intestine with quantitative lineage tracing to reveal the mechanisms of formation and differentiation of villus smooth muscle cells. Within the highly regenerative villus, we uncover a local hierarchy of subepithelial fibroblast progenitors that progress to become mature smooth muscle fibers, via an intermediate contractile myofibroblast-like phenotype, a long-studied hallmark of wound healing. This continuum persists in the adult intestine as the major source of smooth muscle reservoir capable of continuous self-renewal throughout life. We further discover that the NOTCH3-DLL4 signaling axis governs the assembly of villus smooth muscles alongside their adjacent lacteal, which is necessary for gut absorptive function. Overall, our data shed light on the genesis of a poorly defined class of intestinal smooth muscle and pave the way for new opportunities to accelerate recovery of digestive function by stimulating muscle repair.

One Sentence Summary

Villus smooth muscles arise and renew via local myofibroblast-like intermediates governed by the NOTCH3-DLL4 signaling axis

Introduction

The mammalian intestine is a self-renewing organ that processes ingested food, absorbing nutrients from a sea of biochemical, mechanical, and pathogenic insults. Absorption is driven by highly coordinated muscular contractions, which rely on spatiotemporal patterning and functional heterogeneity of intestinal smooth muscle (SM) cells (*1–3*). For fatty nutrients, specialized SM fibers in the intestinal villus contract to propel dietary fats through the central lymphatic capillary, known as the lacteal (**Fig. 1A**) (*1, 2, 4–8*). Whereas most lymphatic capillaries in the body lack SM coverage, the abundance of SM fibers surrounding the lacteal is a unique feature of the contractile villus.

Villus SM cells were first identified in ultrastructural studies in 1909 (*9*) and were subsequently shown to drive villus contractions that intensify in response to dietary fats (*10, 11*). More recent *in vivo* imaging in mice has revealed that villus SM cells facilitate lipid transport by squeezing the adjacent lacteal (*2*). In addition to their contractile function, a subset of villus SM cells secretes VEGFC, the critical lymphatic morphogen. Inducible loss of either *VegfC* or its lacteal-associated receptor *Vegfr3* leads to lacteal regression and impaired dietary fat uptake (*12*).

Unlike most quiescent adult cells, gut villus lacteals and their host intestinal epithelium are in a continuous state of renewal throughout adulthood (*13, 14*). This unique feature of the villus reflects the need to self-repair because the gut is constantly challenged by invasive bacteria, chemical agents, and physical constraints of peristalsis (*1, 13*). Despite the crucial interplay between muscle and lymphatics within this highly regenerative villus, it remains undefined how villus SM cells form, how they assemble alongside lacteals, and how they self-renew to maintain organ homeostasis throughout adult life.

To study these mechanisms, we built a single-cell gene expression atlas of the developing and postnatal mouse intestine across key developmental stages. We reconstructed the transcriptional lineage of intestinal musculature to reveal molecular heterogeneity within intestinal SM cells that are reflective of their distinct anatomical location and function, providing novel molecular markers for their isolation and discrimination. Using inducible lineage tracing, we quantified the dynamics of villus SM differentiation and uncovered a local hierarchy of subepithelial fibroblast and myofibroblast intermediates, characterized by expression of PDGFRα (platelet-derived growth factor receptor alpha) and TNC (Tenascin C), which drive the formation of SM fibers in the perinatal and adult intestine in a process that resembles wound repair (*15*). We find NOTCH3 specifically expressed along this precursor continuum with its receptor DLL4 restricted to the villus capillary vasculature. Using genetic perturbations in mice, we demonstrate that this NOTCH3-DLL4 signaling axis is a contact-dependent mechanism that governs the morphogenesis of the muscular-lacteal complex, which ultimately affects muscular contractility and gut absorptive function. Collectively, our data significantly advance our understanding of the origin and renewal of the muscular-lacteal complex, a system that ensures nutrition throughout life and prevents debilitating digestive and metabolic disorders.

Results

A single-cell RNA-sequencing atlas of the mouse intestinal musculature

To understand the heterogeneity of diverse cell types within the developing intestinal musculature we performed single-cell RNA sequencing (scRNA-seq) to profile the mouse intestine across key developmental stages: embryonic day (E) 12.5, 14.5, 16.5, 18.5, and postnatal day (P) 1.5 (**Fig. 1B**). This time window corresponds to the major transformation of the embryonic gut tube into a functional intestine ready to process fats from maternal milk at birth. We clustered 37,277 high-quality single-cell transcriptomes and used differential gene expression analysis (DGEA) and canonical markers to assign cell-type labels (**Fig. 1, C, D and E, and Fig. S1, A and B, and table S1**). Our data reveal distinct developmental trajectories of progenitor, transitioning, and differentiated cells across all major lineages including intestinal mesenchyme, endothelium, epithelium, mesothelium, enteric nervous system, and circulating blood and immune cells (**Fig. 1, C and E, and Fig. S1C**). Across the distinct lineage clusters, we calculated RNA velocity (*16*) by quantifying the proportion of molecules derived from spliced and unspliced transcripts (**Fig. S1D**). RNA velocity analyses revealed trajectories from early embryonic stage E12.5 to postnatal stage P1.5 (**Fig. 1D**), with evidence of progressive differentiation along each lineage from progenitor cell states at earlier developmental stages, toward mature cells at later time points (**Fig. 1E, top-right panel, and Fig. S1, E and F**).

To reconstruct the developmental trajectory of intestinal musculature, we specifically re-clustered 9,445 mesenchymal cells from the scRNA-seq data to further understand their transcriptional heterogeneity (**Fig. S2, A and B**). To focus our analyses on the absorptive small intestine, we excluded large intestine transcriptomes expressing *Hoxa9*, *Hoxd9*, *Colec10*, and *Adamdec1* (**Fig. S2C**) (*17, 18*). This approach resulted in 7,519 cells across distinct groups

spanning mesenchymal progenitors to mature SM cells across all developmental stages (**Fig. 2, A, B, C, and D, and table S2**). Within these groups, we found three clusters of mature SM cells (SM-1, SM-2, SM-3) that expressed canonical SM markers - Myosin heavy chain 11 (*Myh11*), alpha SM actin (gene: *Acta2*^{high}/protein nomenclature: SMA), and Transgelin (*Tagln*) (**Fig. 2, A and B**) (*8, 19–22*).

Mature SM cells of the small intestine include a heterogeneous mix of villus SM within the *muscularis mucosa* and the two layers of circular and longitudinal muscles of the *muscularis externa* (gut wall) (**Fig. 2A**) (*23*). These populations differentiate radially in sequence during intestinal development, with the outer circular muscle layer developing first, followed by the longitudinal muscle layer, and finally the villus SM fibers arising with lacteal formation close to birth (*8, 24*). This sequence was evident within our unsupervised clustering, with each of the three muscle clusters exhibiting unique transcriptional signatures (**Fig. 2, A, B and D, and Fig. S2E**), and distinct developmental stage composition (**Fig. 2, A and C**). SM-1 and SM-2 contained cells mostly from E12.5 and E14.5 (**Fig. 2, A and C**), consistent with the stepwise differentiation pattern of the emerging gut wall (*8*). In contrast, SM-3 contained cells mostly from P1.5, indicating villus SM identity (**Fig. 2, A and C**) (*24*). Several findings further support these classifications. In a cluster along the trajectory of gut wall progenitors of SM-1 and SM-2, but not SM-3, we found an enrichment of *c-Kit* and other markers of Interstitial Cells of Cajal (ICC) (*1, 25*), which are known to be spatially restricted to the *muscularis externa* (**Fig. 2, A and B**). Forkhead box protein p2 (*Foxp2*) and Neuropilin 2 (*Nrp2*) transcripts were also differentially expressed in the *muscularis externa* (**Fig. 2B and Fig. S3A**).

Using immunofluorescence to validate the spatial fidelity of our cell type classifications in mouse intestinal tissue, we found nuclear-localized FOXP2 protein expression in SMA+ cells of the gut wall but not in the villus (**Fig. 2E**), consistent with SM-1 and SM-2 representing gut wall musculature. Immunofluorescence also confirmed NRP2 expression in the *muscularis externa*, in addition to its previously described expression in the lymphatic endothelium (**Fig. S3A**) (*26*). Together, our transcriptomic analysis captured the differentiation of gut mesenchyme into the diverse musculature of the gut wall and the villus stroma.

Villus SM cells arise from SMA^{low} star cells by PDGFRα+ fibroblast-to-myofibroblast transition

Platelet-derived growth factor receptor alpha (PDGFRα) has recently emerged as a marker of mesenchymal stem and progenitor cells across multiple organ systems (*27*). During villus formation, PDGFRα+ mesenchymal cells accumulate beneath the endoderm forming a subepithelial fibroblast cell population (**Fig. S3B**) (*28–34*). In our transcriptomes from the intestinal musculature, we found *Pdgfrα* expression in mesenchymal progenitor clusters at E12.5 and 14.5, and in a fibroblast-like cluster from later (perinatal) time points (E16.5, E18.5, and P1.5) marked by Periostin (*Postn^{high}*) (**Fig. 2, A, B and C**). In contrast, *Pdgfrα* was absent in mature SMs, ICCs, and a pericyte cell cluster marked by *Cspg4* and *Pdgfrβ^{high}* (**Fig. 2, A and B**) (*22*). Using two-dimensional (2D) scatter plots of our transcriptomes from the *muscularis mucosa*, we observed a stark inverse relationship between the expression of *Pdgfrα* and *Acta2*, while cells expressing *Pdgfrα* and *Myh11* were almost mutually exclusive (**Fig. S3C**). Interestingly, whereas the *Pdgfrα+* fibroblast-like cluster was broadly negative for *Acta2*, we noted a subset of cells that

were $Acta2^{low}$ (**Fig. 2, A and B**), suggesting a cell state transition from fibroblast to myofibroblast, a key step in wound healing (*19, 35–37*).

During physiological wound healing, fibroblast cells progress through a precursor stage to become contractile myofibroblasts, by gradually expressing SMA, arranged as stress fibers (*35, 38, 39*). In our previous studies of the villus SM (*24*), we detected a subset of SMA^{low} villus mesenchymal cells with stellate morphology, which we called star cells, and hypothesized that they represent a precursor state for villus SM differentiation in the embryonic and postnatal intestine. Using immunofluorescence to validate these expression patterns, we found PDGFRα protein in undifferentiated mesenchymal cells just beneath the gut endoderm at E12.5 and E14.5 (**Fig. 2F and Fig. S3D**). At E18.5 and P9, immunofluorescence confirmed PDGFRα expression in the villus subepithelial cells that were closely positioned to, but distinct from the mature (SMA^{high}) SM cells, whereas SMA^{low} star cells displayed variable levels of PDGFRα expression (**Fig. 2F and Fig. S3E**).

Based on these patterns, we hypothesized that during late embryogenesis, *Pdgfrα+* fibroblast-to-myofibroblast transition represents a hierarchical continuum of stem and progenitor cell states involved in villus SM differentiation. To test this, we performed *Pdgfrα+* lineage tracing using the *Pdgfrα-CreERT2* driver (*40*) and *Rosa26-tdTomato* reporter mice (*41*) prior to the formation of star cells (E15.5). This resulted in tdTomato labeling of SMA^{low} star cells in the villus stroma at E18.5 (**Fig. 2G**). Next, we induced *Pdgfrα+* lineage tracing at P0 and collected tissues at P9 (P0i-P9c) to quantify the contribution of the *Pdgfrα+* lineage to the formation of mature SM fibers (**Fig. 3A**). We observed *Pdgfrα+* lineage reporter tdTomato expression in 87 ± 3.4 % of villus SM fibers (**Fig. 3, B and C**). In the next two induction intervals (P9i-P18c and P18i-P27c, **Fig. 3A**), the *Pdgfrα+* lineage contributed to 7.9 ± 0.72 % and 6.3 ± 3.6 % of the SM fibers,

respectively (**Fig. 3, B and C**). Altogether, these data suggest that during the mouse perinatal development, $Pdgfr\alpha+$ fibroblast progenitors progress to become SMA^{low} myofibroblast-like cells that differentiate into villus SM cells.

Villus SM cells renew from TNC+ intestinal myofibroblasts

The transition from fibroblasts to contractile myofibroblasts is paramount to organogenesis, tissue repair, and cancer, but the mechanisms that govern this transition are poorly understood. To investigate the transcriptional changes during the formation of SMA^{low} star cells (a fibroblast-to-myofibroblast transition), we performed unsupervised clustering of the 1,708 perinatal fibroblast-like cells we had captured (**Fig. 2C**). This partitioned them into four groups based on their transcriptomic programs (**Fig. S4A**). Surprisingly, we found that previously described gene expression signatures that define mature fibroblast heterogeneity in the adult villus (*22, 30, 34, 42–47*) could not explain the results of unsupervised clustering of perinatal fibroblasts (**Fig. S4, B, C and D**). Instead, we observed the expression of additional regulators of the fibroblast-to-myofibroblast transition including Palladin (*Palld*) (*48*), Desmin (*Des*) (*49*), transforming growth factor beta-induced (*Tgfβi*) (*50*), and Tenascin-C (*Tnc*) (*51, 52*) (**Fig. S4E**).

TNC is an extracellular matrix protein that can induce actin stress fibers during fibroblast-to-myofibroblast transition (*51, 52*) and has previously been detected in subepithelial myofibroblast cells of the adult villus (*14, 53, 54*). In our scRNA-seq analysis, 2D scatter plots revealed that Tnc expression is low in $Pdgfr\alpha^{high}$ perinatal fibroblasts but peaks in $Pdgfr\alpha^{low}$ and $Acta2^{low}$ myofibroblast intermediates, commensurate with the appearance of the SMA^{low} star cells in the villus (*24*), while mature SM cells expressing Myh11 are rarely Tnc+ (**Fig. 3D**). Immunofluorescence validated these expression patterns by demonstrating TNC protein in SMA^{low}

cells at E18.5 and P9, but not in mature SM fibers (**Fig. 3E and Fig. S4F**). Together, these data suggest that during villus SM differentiation, *Pdgfrα+* fibroblast progenitors transition through a *Tnc+/Acta2^low^* myofibroblast precursor cell state, equivalent to star cells we have described previously (*24*).

To assess the fate of Tnc+ cells in the perinatal stages, we performed lineage tracing using the *Tnc-CreERT2* driver (*55*) at fixed induction-collection intervals, as above (**Fig. 3A**). *TdTomato* expression was observed in 87±4%, 54±4.5%, and 57±5.7% of SM fibers in the induction-collection intervals P0i-P9c, P9i-P18c, and P18i-P27c, respectively (**Fig. 3, F and G**). As expected, *Tnc+* lineage also marked myofibroblast-like cells which were often closely associated with SM fibers (**Fig. 3F**, asterisks). Interestingly, whereas the contribution of *Pdgfrα+* and *Tnc+* lineages to villus SMs cells was comparable at the induction-collection interval of P0i-P9c (87±4% vs. 87±3.4%), the *Tnc+* lineage contribution at later induction times was higher than that of the *Pdgfrα+* lineage contribution (57±5.7% vs. 6.3±3.6% at P18i-P27c). This difference suggests that *Tnc+* myofibroblast-like precursors persist in the mature intestine as a renewable pool of adult SM stem/progenitor cells. Collectively, we conclude that villus SM cells develop from *Tnc+* myofibroblast-like precursors that arise from the *Pdgfrα+* lineage (**Fig. 3H**).

NOTCH3-DLL4 is necessary for the assembly of villus SM cells alongside lacteals

Villus SM cells arise in parallel with the formation of lacteals (E18.5) to generate the muscular-lacteal complex (*24*). Despite its essential function in fat absorption, the mechanisms that govern the assembly of these adjacent cells remain unknown. As part of our effort to understand the molecular nature of the muscular-lacteal interaction, we noted that the juxtracrine (contact-dependent) signaling receptor *Notch3* was strongly enriched in Tnc+ myofibroblasts and villus SM

cells (**Fig. 4A**). In further support of active NOTCH signaling within the muscularis mucosa, we found additional components of this pathway such as *Notch1*, *Jagged1*, and *Hey2* (**Fig. 4A**) (*56*). While most studies focus on the actions of NOTCH signaling in the endothelium, *Notch3* is the predominant NOTCH receptor responsible for vascular SM maturation and is the causal gene for the hereditary vascular dementia CADASIL, characterized by degeneration of SM cells (*57–59*). In our 2D scatter plots, *Notch3* levels were correlated with *Acta2* and *Myh11* expression, consistent with NOTCH signaling activity along the myofibroblast-to-villus SM trajectory (**Fig. 4B**). Through immunofluorescence at E18.5 and P9, we confirmed NOTCH3 protein expression in SMA^{low} star cells and in SMA^{high} mature SM fibers (**Fig. 4C**). We also validated protein expression of Hairy/enhancer-of-split related with YRPW motif protein 2 (HEY2, **Fig. 4A and S5A**) and Melanoma cell adhesion molecule (MCAM, **Fig. 4A and Fig. S5B**) whose activities are also associated with a vascular SM phenotype (*60–62*).

NOTCH is a short-range signaling pathway that occurs between membrane-bound receptors and ligands expressed on adjacent cells. Of interest, the Notch ligand Delta-like 4 (DLL4) is highly expressed in tip cells of sprouting lacteals where it directs filopodia-mediated lacteal survival and regeneration (*14*). We validated DLL4 expression in the perinatal lacteal tip cells using the lymphatic endothelial cell marker LYVE1 (*63*) and Prox1-GFP lymphatic reporter mice (*64*) (**Fig. 4D and Fig. S5C**) and hypothesized that contact-dependent NOTCH3-DLL4 signaling is necessary for the assembly of the muscular-lacteal complex. To test this, we deleted *Notch3* or *Dll4* from villus SM, or lymphatic endothelial cells, respectively (*65*, *66*). Deleting *Notch3* at P0 (with *Pdgfrα-CreERT2*) (**Fig. 4, E and F**) or in the embryonic gut mesenchyme (**Fig S5D**) (with *Hoxb6-Cre*) (*67*) resulted in a significant reduction in the height of villus SM fibers at P9 (**Fig. S5E and Fig. S6, A and B**). A similar reduction in the length of SM fibers was observed when

Dll4 was removed from lacteals (P0, with *Prox1-CreERT2*) (*68*) (**Fig. 4F and Fig. S6C**). Muscle fibers were not extended beyond their adjacent lacteal tip in 28% of the villi upon *Notch3* deletion at P0 (**Fig. 4, E and G**), in 37.3% using *Hoxb6-cre* (**Fig. S5D**), and in 26.7% when *Dll4* was deleted from lacteals (**Fig. 4G**). This was statistically significant when compared to control mice where most muscle fibers (> 96%) extended beyond lacteals (**Fig. 4G and Fig. S5D**). *Notch3* deletion from the musculature had no effect on lacteal length (**Fig. S6, D and E**), but *Dll4* deletion from lacteals reduced lacteal length ($\leq$ 20% villus length) with 17.3% of the mutant villi developing without lacteals (**Fig. S6F**), consistent with prior findings (*14*). Finally, deletion of either *Notch3* or *Dll4* resulted in a 40-50% reduction in the number of lacteal filopodia (**Fig. S6, G, H, and I**) (*14*). Together, these results indicate that NOTCH3-DLL4 signaling governs the assembly of villus SM fibers alongside their adjacent lacteals (**Fig. 4H**).

Discussion

Intestinal villi are the fundamental units of nutrient absorption and transport that constantly regenerate to withstand the hostile conditions of the digestive tract. Villus SM fibers drive villus movement and contractility to propel lipid drainage through the lymphatic lacteals (*2, 4, 5*). Unlike other cell types of the intestine, such as the epithelium, the mesenchyme lacks gene expression data and genetic tools and has prevented us from understanding the mechanisms that pattern intestinal SM during development and regeneration. To address this gap in knowledge, we created a time-resolved transcriptomic atlas of mouse intestinal development capturing the diversity of intestinal cell lineages at key embryonic and postnatal stages. From these data we reconstructed the trajectory of mesenchymal differentiation that produces the musculature of the gut wall and villus stroma.

Muscle cell contractile activity and their eventual breakdown belies the constant muscle renewal within organs, a function performed by adult stem cells. Satellite cells are one well-studied example that maintain skeletal muscle homeostasis (*69*), but similar mechanisms driving assembly and maintenance of intestinal SM remained undefined. Ultrastructural and genetic studies have detected distinct mesenchymal cell morphologies surrounding villus SM fibers (*24, 70–72*), and this villus mesenchyme has crucial roles in the zonation, maintenance, and renewal of the intestinal epithelium (*22, 30, 34, 43, 47, 53, 70, 73, 74*). However, the role of the mesenchyme in villus SM maintenance and renewal had not been explored. Our current findings suggest that villus SM cells differentiate from PDGFRα+ fibroblasts in the villus. By inducing lineage tracing in multiple pulse-chase intervals in embryonic and juvenile mice, we found that villus mesenchymal fibroblasts undergo a myofibroblast-like transition during differentiation towards contractile villus SM. In both *Pdgfrα+* and *Tnc+* cell lineage tracing, tdTomato contribution to SM fibers was greater in the P0i-P9c interval compared to the P9i-P18c and P18i-P27c intervals (**Fig. 3, C and G**). These rates likely reflect villus SM assembly starting at birth (in the P0i-P9c interval) and shifting toward regenerative turnover by the next two induction intervals (P9i-P18c and P18i-P27c). In the adult mouse intestine, villus mesenchymal cells are non-uniformly distributed along the crypt-villus axis where PDGFRα^{high} cells are concentrated closer to the villus crypt and are less frequent along the rest of the villus (*34*). TNC expression has been reported to be specific to fibroblasts in the villus subepithelial layer but absent in the crypt (*14, 53*). We interpret this to mean that in the highly regenerative villus, a majority of the adult subepithelial fibroblasts are committed as TNC+ myofibroblast-like cells, ready for villus SM fiber renewal. Hence, therapeutic targeting of myofibroblast intermediates may prove to be a viable strategy for enhancing the repair of intestinal SM.

Villus SM cells assemble as axial fibers, closely associated with the lacteal during perinatal development, and their interactions are critical for absorbing dietary lipids (*2, 5*). Villus SM cells are a major source of VEGFC, the critical lymphangiogenic growth factor necessary for lacteal maintenance and lipid absorption (*12*). Genetic mutations in the embryonic mesoderm can disrupt the structure of both the villus SM and their adjacent lacteals (*24*). However, the reciprocal mechanisms guiding villus SM assembly alongside lacteals have not been described. Our work uncovers a specific upregulation of NOTCH3 signaling and a vascular SM-like gene expression signature in villus SM. DLL4 expression in lacteal tip cells is necessary for adult lacteal regeneration and proper lipid transport (*14*) - hence, NOTCH3 expression in the villus SM suggested contact-dependent signaling within the muscular-lacteal complex. We found that the villus muscular-lacteal complex of juvenile mice failed to properly assemble when *Notch3* was removed from their mesenchymal cells or when *Dll4* was removed from their lymphatic endothelium. Whereas loss of *Dll4* resulted in a reduction in the length of both the lacteals and the villus SM, *Notch3* loss in the mesenchyme affected only the villus SM length. We also observed a reduction in the percentage of lacteals that possessed tip cell filopodia upon the loss of either *Notch3* or *Dll4*. These findings uncover a previously unknown role for NOTCH3-DLL4 signaling in the morphogenesis of the muscular-lacteal complex and function in fat absorption. NOTCH3 signaling regulates the maturation of vascular SM cells in visceral organ arteries and cell-autonomously controls the differentiation of the DLL4+ arterial endothelial cells (*57, 58, 62, 75, 75–77*). When we removed *Notch3* from the mesenchymal cells, we also observed a loss of vascular SM coverage on the major blood vessels of the gut dorsal mesentery (**Fig. S6J**), suggesting that Notch3 is a global regulator of gut vascular SM. Moreover, these data suggest that during the *de novo* generation of the mucosal musculature, the myofibroblast-like transition of

local fibroblasts generates the villus SM in phenotypic continuity with the vascular SM of the mesenteric blood vessels. Thus, mammalian lacteals may have co-opted the use of DLL4+ expression in their tip cells to enable muscular-lacteal coupling and assembly. Collectively, our findings reveal the molecular and cellular mechanism of villus SM morphogenesis and renewal, and serve as a framework for understanding the developmental specification, organization, and renewal of intestinal mesenchyme.

References and notes

1. K. M. Sanders, S. D. Koh, S. Ro, S. M. Ward, Regulation of gastrointestinal motility—insights from smooth muscle biology. *Nat. Rev. Gastroenterol. Hepatol.* **9**, 633–645 (2012).

2. K. Choe, J. Y. Jang, I. Park, Y. Kim, S. Ahn, D. Y. Park, Y. K. Hong, K. Alitalo, G. Y. Koh, P. Kim, Intravital imaging of intestinal lacteals unveils lipid drainage through contractility. *J. Clin. Invest.* **125**, 4042–4052 (2015).

3. N. C. Joyce, M. F. Haire, G. E. Palade, Morphologic and biochemical evidence for a contractile cell network within the rat intestinal mucosa. *Gastroenterology*. **92**, 68–81 (1987).

4. C. T. Phan, P. Tso, Intestinal lipid absorption and transport. *Front. Biosci.-Landmark*. **6**, 299–319 (2001).

5. J. B. Dixon, Mechanisms of chylomicron uptake into lacteals. *Ann. N. Y. Acad. Sci.* **1207**, E52–E57 (2010).

6. V. A. McLin, S. J. Henning, M. Jamrich, The Role of the Visceral Mesoderm in the Development of the Gastrointestinal Tract. *Gastroenterology*. **136**, 2074–2091 (2009).

7. R. T. Thomason, D. M. Bader, N. I. Winters, Comprehensive timeline of mesodermal development in the quail small intestine. *Dev. Dyn.* **241**, 1678–1694 (2012).

8. T. R. Huycke, B. M. Miller, H. K. Gill, N. L. Nerurkar, D. Sprinzak, L. Mahadevan, C. J. Tabin, Genetic and Mechanical Regulation of Intestinal Smooth Muscle Development. *Cell*. **179**, 90-105.e21 (2019).

9. A. Trautman, Die Muskulatur in den Dünndarmzotten der Haustiere. *Anat. Anz.*, 113–125.

10. J. S. Lee, Contraction of villi and fluid transport in dog jejunal mucosa in vitro. *Am. J. Physiol.* **221**, 488–495 (1971).

11. W. A. Womack, P. K. Tygart, D. Mailman, P. R. Kvietys, D. N. Granger, Villous motility: Relationship to lymph flow and blood flow in the dog jejunum. *Gastroenterology*. **94**, 977–983 (1988).

12. H. Nurmi, P. Saharinen, G. Zarkada, W. Zheng, M. R. Robciuc, K. Alitalo, VEGF -C is required for intestinal lymphatic vessel maintenance and lipid absorption. *EMBO Mol. Med.* **7**, 1418–1425 (2015).

13. L. G. van der Flier, H. Clevers, Stem Cells, Self-Renewal, and Differentiation in the Intestinal Epithelium. *Annu. Rev. Physiol.* **71**, 241–260 (2009).

14. J. Bernier-Latmani, C. Cisarovsky, C. S. Demir, M. Bruand, M. Jaquet, S. Davanture, S. Ragusa, S. Siegert, O. Dormond, R. Benedito, F. Radtke, S. A. Luther, T. V. Petrova, DLL4 promotes continuous adult intestinal lacteal regeneration and dietary fat transport. *J. Clin. Invest.* **125**, 4572–4586 (2015).

15. R. Schuster, F. Younesi, M. Ezzo, B. Hinz, The Role of Myofibroblasts in Physiological and Pathological Tissue Repair. *Cold Spring Harb. Perspect. Biol.*, a041231 (2022).

16. G. La Manno, R. Soldatov, A. Zeisel, E. Braun, H. Hochgerner, V. Petukhov, K. Lidschreiber, M. E. Kastriti, P. Lönnerberg, A. Furlan, J. Fan, L. E. Borm, Z. Liu, D. van Bruggen, J. Guo, X. He, R. Barker, E. Sundström, G. Castelo-Branco, P. Cramer, I. Adameyko, S. Linnarsson, P. V. Kharchenko, RNA velocity of single cells. *Nature*. **560**, 494–498 (2018).

17. Y. Kawazoe, T. Sekimoto, M. Araki, K. Takagi, K. Araki, K. Yamamura, Region-specific gastrointestinal Hox code during murine embryonal gut development. *Dev. Growth Differ.* **44**, 77–84 (2002).

18. S. E. Ha, B. G. Jorgensen, L. Wei, B. Jin, M.-S. Kim, S. M. Poudrier, R. Singh, A. Bartlett,

H. Zogg, S. Kim, G. Baek, M. Kurahashi, M.-Y. Lee, Y.-S. Kim, S.-C. Choi, K. C. Sasse, S. J. S. Rubin, A. Gottfried-Blackmore, L. Becker, A. Habtezion, K. M. Sanders, S. Ro, Metalloendopeptidase ADAM-like Decysin 1 (ADAMDEC1) in Colonic Subepithelial PDGFRα+ Cells Is a New Marker for Inflammatory Bowel Disease. *Int. J. Mol. Sci.* **23**, 5007 (2022).

19. B. Hinz, G. Celetta, J. J. Tomasek, G. Gabbiani, C. Chaponnier, Alpha-smooth muscle actin expression upregulates fibroblast contractile activity. *Mol. Biol. Cell* (2001), doi:10.1091/mbc.12.9.2730.

20. J. M. Miano, P. Cserjesi, K. L. Ligon, M. Periasamy, E. N. Olson, Smooth muscle myosin heavy chain exclusively marks the smooth muscle lineage during mouse embryogenesis. *Circ. Res.* **75**, 803–812 (1994).

21. L. Li, J. M. Miano, P. Cserjesi, E. N. Olson, SM22α, a Marker of Adult Smooth Muscle, Is Expressed in Multiple Myogenic Lineages During Embryogenesis. *Circ. Res.* **78**, 188–195 (1996).

22. N. McCarthy, J. Kraiczy, R. A. Shivdasani, Cellular and molecular architecture of the intestinal stem cell niche. *Nat. Cell Biol.* **22**, 1033–1041 (2020).

23. G. Gabella, On the musculature of the gastro-intestinal tract of the guinea-pig. *Anat. Embryol. (Berl.)*. **163**, 135–156 (1981).

24. S. Hu, A. Mahadevan, I. F. Elysee, J. Choi, N. R. Souchet, G. H. Bae, A. K. Taboada, B. Sanketi, G. E. Duhamel, C. S. Sevier, G. Tao, N. A. Kurpios, The asymmetric Pitx2 gene regulates gut muscular-lacteal development and protects against fatty liver disease. *Cell Rep.* **37** (2021), doi:10.1016/j.celrep.2021.110030.

25. K. M. Sanders, S. M. Ward, S. D. Koh, Interstitial Cells: Regulators of Smooth Muscle

Function. *Physiol. Rev.* **94**, 859–907 (2014).

26. Y. Xu, L. Yuan, J. Mak, L. Pardanaud, M. Caunt, I. Kasman, B. Larrivée, R. del Toro, S. Suchting, A. Medvinsky, J. Silva, J. Yang, J.-L. Thomas, A. W. Koch, K. Alitalo, A. Eichmann, A. Bagri, Neuropilin-2 mediates VEGF-C–induced lymphatic sprouting together with VEGFR3. *J. Cell Biol.* **188**, 115–130 (2010).

27. R. M. Farahani, M. Xaymardan, Platelet-Derived Growth Factor Receptor Alpha as a Marker of Mesenchymal Stem Cells in Development and Stem Cell Biology. *Stem Cells Int.* **2015**, 362753 (2015).

28. K. D. Walton, Å. Kolterud, M. J. Czerwinski, M. J. Bell, A. Prakash, J. Kushwaha, A. S. Grosse, S. Schnell, D. L. Gumucio, Hedgehog-responsive mesenchymal clusters direct patterning and emergence of intestinal villi. *Proc. Natl. Acad. Sci. U. S. A.* **109**, 15817–15822 (2012).

29. A. Rao-Bhatia, M. Zhu, W. C. Yin, S. Coquenlorge, X. Zhang, J. Woo, Y. Sun, C. H. Dean, A. Liu, C. chung Hui, R. A. Shivdasani, H. McNeill, S. Hopyan, T. H. Kim, Hedgehog-Activated Fat4 and PCP Pathways Mediate Mesenchymal Cell Clustering and Villus Formation in Gut Development. *Dev. Cell*. **52**, 647-658.e6 (2020).

30. G. Greicius, PDGFRalpha(+) pericryptal stromal cells are the critical source of Wnts and RSPO3 for murine intestinal stem cells in vivo. *Proc Natl Acad Sci USA*. **115**, E3173–E3181 (2018).

31. L. Karlsson, P. Lindahl, J. K. Heath, C. Betsholtz, Abnormal gastrointestinal development in PDGF-A and PDGFR-(alpha) deficient mice implicates a novel mesenchymal structure with putative instructive properties in villus morphogenesis. *Development*. **127**, 3457–3466 (2000).

32. M. Maimets, M. T. Pedersen, J. Guiu, J. Dreier, M. Thodberg, Y. Antoku, P. J. Schweiger, L. Rib, R. B. Bressan, Y. Miao, K. C. Garcia, A. Sandelin, P. Serup, K. B. Jensen, Mesenchymal-epithelial crosstalk shapes intestinal regionalisation via Wnt and Shh signalling. *Nat. Commun. 2022 131*. **13**, 1–12 (2022).

33. M. Kurahashi, Y. Nakano, L. E. Peri, J. B. Townsend, S. M. Ward, K. M. Sanders, A novel population of subepithelial platelet-derived growth factor receptor α-positive cells in the mouse and human colon. *Am. J. Physiol. - Gastrointest. Liver Physiol.* **304**, G823–G834 (2013).

34. N. McCarthy, E. Manieri, E. E. Storm, A. Saadatpour, A. M. Luoma, V. N. Kapoor, S. Madha, L. T. Gaynor, C. Cox, S. Keerthivasan, K. Wucherpfennig, G. C. Yuan, F. J. de Sauvage, S. J. Turley, R. A. Shivdasani, Distinct Mesenchymal Cell Populations Generate the Essential Intestinal BMP Signaling Gradient. *Cell Stem Cell*. **26**, 391-402.e5 (2020).

35. B. Hinz, V. Dugina, C. Ballestrem, B. Wehrle-Haller, C. Chaponnier, α-Smooth Muscle Actin Is Crucial for Focal Adhesion Maturation in Myofibroblasts. *Mol. Biol. Cell*. **14**, 2508–2519 (2003).

36. B. Hinz, G. Gabbiani, Mechanisms of force generation and transmission by myofibroblasts. *Curr. Opin. Biotechnol.* **14**, 538–546 (2003).

37. L. Yao, B. H. Rathnakar, H. R. Kwon, H. Sakashita, J. H. Kim, A. Rackley, J. J. Tomasek, W. L. Berry, L. E. Olson, Temporal control of PDGFRα regulates the fibroblast-to-myofibroblast transition in wound healing. *Cell Rep.* **40**, 111192 (2022).

38. B. Hinz, S. H. Phan, V. J. Thannickal, A. Galli, M.-L. Bochaton-Piallat, G. Gabbiani, The Myofibroblast: One Function, Multiple Origins. *Am. J. Pathol.* **170**, 1807–1816 (2007).

39. J. J. Tomasek, G. Gabbiani, B. Hinz, C. Chaponnier, R. A. Brown, Myofibroblasts and

mechano-regulation of connective tissue remodelling. *Nat. Rev. Mol. Cell Biol.* **3**, 349–363 (2002).

40. M.-I. Chung, M. Bujnis, C. E. Barkauskas, Y. Kobayashi, B. L. M. Hogan, Niche-mediated BMP/SMAD signaling regulates lung alveolar stem cell proliferation and differentiation. *Development*. **145**, dev163014 (2018).

41. L. Madisen, T. A. Zwingman, S. M. Sunkin, S. W. Oh, H. A. Zariwala, H. Gu, L. L. Ng, R. D. Palmiter, M. J. Hawrylycz, A. R. Jones, E. S. Lein, H. Zeng, A robust and high-throughput Cre reporting and characterization system for the whole mouse brain. *Nat. Neurosci.* **13**, 133–140 (2010).

42. W. de Lau, N. Barker, T. Y. Low, B.-K. Koo, V. S. W. Li, H. Teunissen, P. Kujala, A. Haegebarth, P. J. Peters, M. van de Wetering, D. E. Stange, J. van Es, D. Guardavaccaro, R. B. M. Schasfoort, Y. Mohri, K. Nishimori, S. Mohammed, A. J. R. Heck, H. Clevers, Lgr5 homologues associate with Wnt receptors and mediate R-spondin signalling. *Nature*. **476**, 293–297 (2011).

43. B. Degirmenci, T. Valenta, S. Dimitrieva, G. Hausmann, K. Basler, GLI1-expressing mesenchymal cells form the essential Wnt-secreting niche for colon stem cells. *Nat. 2018 5587710*. **558**, 449–453 (2018).

44. L. E. Batts, D. B. Polk, R. N. Dubois, H. Kulessa, Bmp signaling is required for intestinal growth and morphogenesis. *Dev. Dyn.* **235**, 1563–1570 (2006).

45. X. C. He, J. Zhang, W.-G. Tong, O. Tawfik, J. Ross, D. H. Scoville, Q. Tian, X. Zeng, X. He, L. M. Wiedemann, Y. Mishina, L. Li, BMP signaling inhibits intestinal stem cell self-renewal through suppression of Wnt–β-catenin signaling. *Nat. Genet.* **36**, 1117–1121 (2004).

46. F. Kuhnert, C. R. Davis, H.-T. Wang, P. Chu, M. Lee, J. Yuan, R. Nusse, C. J. Kuo, Essential requirement for Wnt signaling in proliferation of adult small intestine and colon revealed by adenoviral expression of Dickkopf-1. *Proc. Natl. Acad. Sci.* **101**, 266–271 (2004).

47. M. Shoshkes-Carmel, Y. J. Wang, K. J. Wangensteen, B. Tóth, A. Kondo, E. E. Massassa, S. Itzkovitz, K. H. Kaestner, Subepithelial telocytes are an important source of Wnts that supports intestinal crypts. *Nat. 2018 5577704*. **557**, 242–246 (2018).

48. M. J. Rönty, S.-K. Leivonen, B. Hinz, A. Rachlin, C. A. Otey, V.-M. Kähäri, O. M. Carpén, Isoform-Specific Regulation of the Actin-Organizing Protein Palladin during TGF-β1-Induced Myofibroblast Differentiation. *J. Invest. Dermatol.* **126**, 2387–2396 (2006).

49. B. Hinz, D. Mastrangelo, C. E. Iselin, C. Chaponnier, G. Gabbiani, Mechanical Tension Controls Granulation Tissue Contractile Activity and Myofibroblast Differentiation. *Am. J. Pathol.* **159**, 1009–1020 (2001).

50. A. Desmouliere, A. Geinoz, F. Gabbiani, G. Gabbiani, Transforming growth factor-β1 induces α-smooth muscle actin expression in granulation tissue myofibroblasts and in quiescent and growing cultured fibroblasts. *J. Cell Biol.* (1993), doi:10.1083/jcb.122.1.103.

51. S. Bhattacharyya, W. Wang, L. Morales-Nebreda, G. Feng, M. Wu, X. Zhou, R. Lafyatis, J. Lee, M. Hinchcliff, C. Feghali-Bostwick, K. Lakota, G. R. S. Budinger, K. Raparia, Z. Tamaki, J. Varga, Tenascin-C drives persistence of organ fibrosis. *Nat. Commun. 2016 71*. **7**, 1–14 (2016).

52. D. Katoh, Y. Kozuka, A. Noro, T. Ogawa, K. Imanaka-Yoshida, T. Yoshida, Tenascin-C Induces Phenotypic Changes in Fibroblasts to Myofibroblasts with High Contractility through the Integrin αvβ1/Transforming Growth Factor β/SMAD Signaling Axis in Human

Breast Cancer. *Am. J. Pathol.* **190**, 2123–2135 (2020).

53. J. Bernier-Latmani, C. Mauri, R. Marcone, F. Renevey, S. Durot, L. He, M. Vanlandewijck, C. Maclachlan, S. Davanture, N. Zamboni, G. W. Knott, S. A. Luther, C. Betsholtz, M. Delorenzi, C. Brisken, T. V. Petrova, ADAMTS18+ villus tip telocytes maintain a polarized VEGFA signaling domain and fenestrations in nutrient-absorbing intestinal blood vessels. *Nat. Commun. 2022 131*. **13**, 1–17 (2022).

54. M. Islam, M. Kusakabe, K. Horiguchi, S. Iino, T. Nakamura, K. Iwanaga, H. Hashimoto, S. Matsumoto, T. Murata, M. Hori, H. Ozaki, PDGF and TGF-β promote tenascin-C expression in subepithelial myofibroblasts and contribute to intestinal mucosal protection in mice. *Br. J. Pharmacol.* **171**, 375–388 (2014).

55. W. He, Q. Xie, Y. Wang, J. Chen, M. Zhao, L. S. Davis, M. D. Breyer, G. Gu, C.-M. Hao, Generation of a Tenascin-C-CreER2 Knockin Mouse Line for Conditional DNA Recombination in Renal Medullary Interstitial Cells. *PLOS ONE*. **8**, e79839 (2013).

56. C. Siebel, U. Lendahl, Notch Signaling in Development, Tissue Homeostasis, and Disease. *Physiol. Rev.* **97**, 1235–1294 (2017).

57. V. Domenga, P. Fardoux, P. Lacombe, M. Monet, J. Maciazek, L. T. Krebs, B. Klonjkowski, E. Berrou, M. Mericskay, Z. Li, E. Tournier-Lasserve, T. Gridley, A. Joutel, Notch3 is required for arterial identity and maturation of vascular smooth muscle cells. *Genes Dev.* **18**, 2730–2735 (2004).

58. Q. Wang, N. Zhao, S. Kennard, B. Lilly, Notch2 and Notch3 Function Together to Regulate Vascular Smooth Muscle Development. *PLOS ONE*. **7**, e37365 (2012).

59. A. Joutel, C. Corpechot, A. Ducros, K. Vahedi, H. Chabriat, P. Mouton, S. Alamowitch, V. Domenga, M. Cécillion, E. Maréchal, J. Maciazek, C. Vayssière, C. Cruaud, E.-A. Cabanis,

M. M. Ruchoux, J. Weissenbach, J. F. Bach, M. G. Bousser, E. Tournier-Lasserve, Notch3 mutations in CADASIL, a hereditary adult-onset condition causing stroke and dementia. *Nature*. **383**, 707–710 (1996).

60. N. Espagnolle, F. Guilloton, F. Deschaseaux, M. Gadelorge, L. Sensébé, P. Bourin, CD146 expression on mesenchymal stem cells is associated with their vascular smooth muscle commitment. *J. Cell. Mol. Med.* **18**, 104–114 (2014).

61. Y. Sakata, F. Xiang, Z. Chen, Y. Kiriyama, C. N. Kamei, D. I. Simon, M. T. Chin, Transcription Factor CHF1/Hey2 Regulates Neointimal Formation In Vivo and Vascular Smooth Muscle Proliferation and Migration In Vitro. *Arterioscler. Thromb. Vasc. Biol.* **24**, 2069–2074 (2004).

62. D. Morrow, S. Guha, C. Sweeney, Y. Birney, T. Walshe, C. O'Brien, D. Walls, E. M. Redmond, P. A. Cahill, Notch and Vascular Smooth Muscle Cell Phenotype. *Circ. Res.* **103**, 1370–1382 (2008).

63. K. E. Kim, H.-K. Sung, G. Y. Koh, Lymphatic development in mouse small intestine. *Dev. Dyn. Off. Publ. Am. Assoc. Anat.* **236**, 2020–2025 (2007).

64. I. Choi, H. K. Chung, S. Ramu, H. N. Lee, K. E. Kim, S. Lee, J. Yoo, D. Choi, Y. S. Lee, B. Aguilar, Y.-K. Hong, Visualization of lymphatic vessels by Prox1-promoter directed GFP reporter in a bacterial artificial chromosome-based transgenic mouse. *Blood*. **117**, 362–365 (2011).

65. T. Nadeem, W. Bogue, B. Bigit, H. Cuervo, Deficiency of Notch signaling in pericytes results in arteriovenous malformations. *JCI Insight*. **5**, e125940.

66. U. Koch, E. Fiorini, R. Benedito, V. Besseyrias, K. Schuster-Gossler, M. Pierres, N. R. Manley, A. Duarte, H. R. MacDonald, F. Radtke, Delta-like 4 is the essential, nonredundant

ligand for Notch1 during thymic T cell lineage commitment. *J. Exp. Med.* **205**, 2515–2523 (2008).

67. L. A. Lowe, S. Yamada, M. R. Kuehn, HoxB6-Cre transgenic mice express Cre recombinase in extra-embryonic mesoderm, in lateral plate and limb mesoderm and at the midbrain/hindbrain junction. *genesis*. **26**, 118–120 (2000).

68. R. S. Srinivasan, M. E. Dillard, O. V. Lagutin, F.-J. Lin, S. Tsai, M.-J. Tsai, I. M. Samokhvalov, G. Oliver, Lineage tracing demonstrates the venous origin of the mammalian lymphatic vasculature. *Genes Dev.* **21**, 2422–2432 (2007).

69. H. Yin, F. Price, M. A. Rudnicki, Satellite Cells and the Muscle Stem Cell Niche. *Physiol. Rev.* **93**, 23–67 (2013).

70. S. P. Hong, M. J. Yang, H. Cho, I. Park, H. Bae, K. Choe, S. H. Suh, R. H. Adams, K. Alitalo, D. Lim, G. Y. Koh, Distinct fibroblast subsets regulate lacteal integrity through YAP/TAZ-induced VEGF-C in intestinal villi. *Nat. Commun. 2020 111*. **11**, 1–16 (2020).

71. Y. Hosoyamada, T. Sakai, Mechanical components of rat intestinal villi as revealed by ultrastructural analysis with special reference to the axial smooth muscle cells in the villi. *Arch. Histol. Cytol.* **70**, 107–116 (2007).

72. S. L. Palay, L. J. Karlin, An Electron Microscopic Study of the Intestinal Villus. *J. Biophys. Biochem. Cytol.* **5**, 363–371 (1959).

73. N. McCarthy, G. Tie, S. Madha, J. Kraiczy, A. Maglieri, R. A. Shivdasani, Delineation and birth of a multi-layer intestinal stem cell niche (2022), p. 2021.09.28.462142, , doi:10.1101/2021.09.28.462142.

74. I. Stzepourginski, G. Nigro, J.-M. Jacob, S. Dulauroy, P. J. Sansonetti, G. Eberl, L. Peduto, CD34 + mesenchymal cells are a major component of the intestinal stem cells niche at

homeostasis and after injury, doi:10.1073/pnas.1620059114.

75. N. M. Kofler, C. J. Shawber, T. Kangsamaksin, H. O. Reed, J. Galatioto, J. Kitajewski, Notch Signaling in Developmental and Tumor Angiogenesis. *Genes Cancer*. **2**, 1106–1116 (2011).

76. L. C. Steffes, A. A. Froistad, A. Andruska, M. Boehm, M. McGlynn, F. Zhang, W. Zhang, D. Hou, X. Tian, L. Miquerol, K. Nadeau, R. J. Metzger, E. Spiekerkoetter, M. E. Kumar, A Notch3-Marked Subpopulation of Vascular Smooth Muscle Cells Is the Cell of Origin for Occlusive Pulmonary Vascular Lesions. *Circulation*. **142**, 1545–1561 (2020).

77. H. Ragot, A. Monfort, M. Baudet, F. Azibani, L. Fazal, R. Merval, E. Polidano, A. Cohen-Solal, C. Delcayre, N. Vodovar, C. Chatziantoniou, J.-L. Samuel, Loss of Notch3 Signaling in Vascular Smooth Muscle Cells Promotes Severe Heart Failure Upon Hypertension. *Hypertension*. **68**, 392–400 (2016).

78. F. A. Wolf, P. Angerer, F. J. Theis, SCANPY: large-scale single-cell gene expression data analysis. *Genome Biol.* **19**, 15 (2018).

79. S. L. Wolock, R. Lopez, A. M. Klein, Scrublet: Computational Identification of Cell Doublets in Single-Cell Transcriptomic Data. *Cell Syst.* **8**, 281-291.e9 (2019).

80. F. A. Wolf, F. K. Hamey, M. Plass, J. Solana, J. S. Dahlin, B. Göttgens, N. Rajewsky, L. Simon, F. J. Theis, PAGA: graph abstraction reconciles clustering with trajectory inference through a topology preserving map of single cells. *Genome Biol.* **20**, 59 (2019).

81. V. Bergen, M. Lange, S. Peidli, F. A. Wolf, F. J. Theis, Generalizing RNA velocity to transient cell states through dynamical modeling. *Nat. Biotechnol.* **38**, 1408–1414 (2020).

82. B. Lizen, M. Claus, L. Jeannotte, F. M. Rijli, F. Gofflot, Perinatal induction of Cre recombination with tamoxifen. *Transgenic Res.* **24**, 1065–1077 (2015).

83. S. Hu, C. S. Sevier, N. A. Kurpios, Protocol to detect smooth muscle actin-alpha and measure oxidative damage in neonatal mouse intestine. *STAR Protoc.* **3**, 101524 (2022).

84. J. Bernier-Latmani, T. V. Petrova, High-resolution 3D analysis of mouse small-intestinal stroma. *Nat. Protoc.* **11**, 1617–1629 (2016).

Acknowledgments

Funding

Autor contributions

BDS, MM, IDV, and NAK designed the study. BDS and MM performed the scRNA-seq experiments and analyzed the data. BDS and MAT performed the WT immunostaining experiments. BDS performed lineage tracing and gene knockout experiments. SH and MFZW

assisted with data analysis and interpretation. BDS, MM, IDV, and NAK wrote the manuscript. All authors provided feedback and comments.

Data and code availability

The authors declare that all sequencing data supporting the findings of this study have been deposited in NCBI's Gene Expression Omnibus with GEO series accession number GSE222122. All code and scripts needed to reproduce the findings of this manuscript have been deposited on GitHub: (https://github.com/madhavmantri/mouse_intestine_development). All other data supporting the findings in this study are included in the main article and associated files.

Conflicts

The authors declare no conflicts.

Supplementary Materials

Materials and Methods

Figs. S1 to S6

Table S1 to S2

Main figure legends

Figure 1: A time-resolved single-cell transcriptomic atlas of mouse intestinal development.

(A) Cartoon depicting the distinct patterning of smooth muscles (SMs) in the gut wall and the villus. The villus contains a fat absorptive complex of lymphatic lacteals and their associated SMs, which drains dietary lipids into the systemic circulation. **(B)** Experimental workflow and analysis for single-cell RNA-sequencing (scRNA-seq) at 5 embryonic and postnatal stages (E12.5, E14.5, E16.5, E18.5, P1.5). **(C)** Uniform manifold approximation and projection (UMAP) plot of 37,277 single-cell transcriptomes from mouse intestine at 5 stages, clustered by gene expression and colored by cell type labels. Partition-based graph abstraction (PAGA) map overlaid on UMAP with circles representing cell types and edges representing global relationships between cell types. **(D)** UMAP plot showing mouse developmental stage of origin and transcriptomic velocity for the intestinal scRNA-seq data. **(E)** Cell type labels segregated based on intestinal cell lineages and UMAP plots showing the expression of selected clusters and cell type gene markers. Dotted lines on UMAP plots encircle transcriptomes with expression. The bar plot in the top panel shows the proportion of cells from cell types in gut musculature lineage across developmental stages.
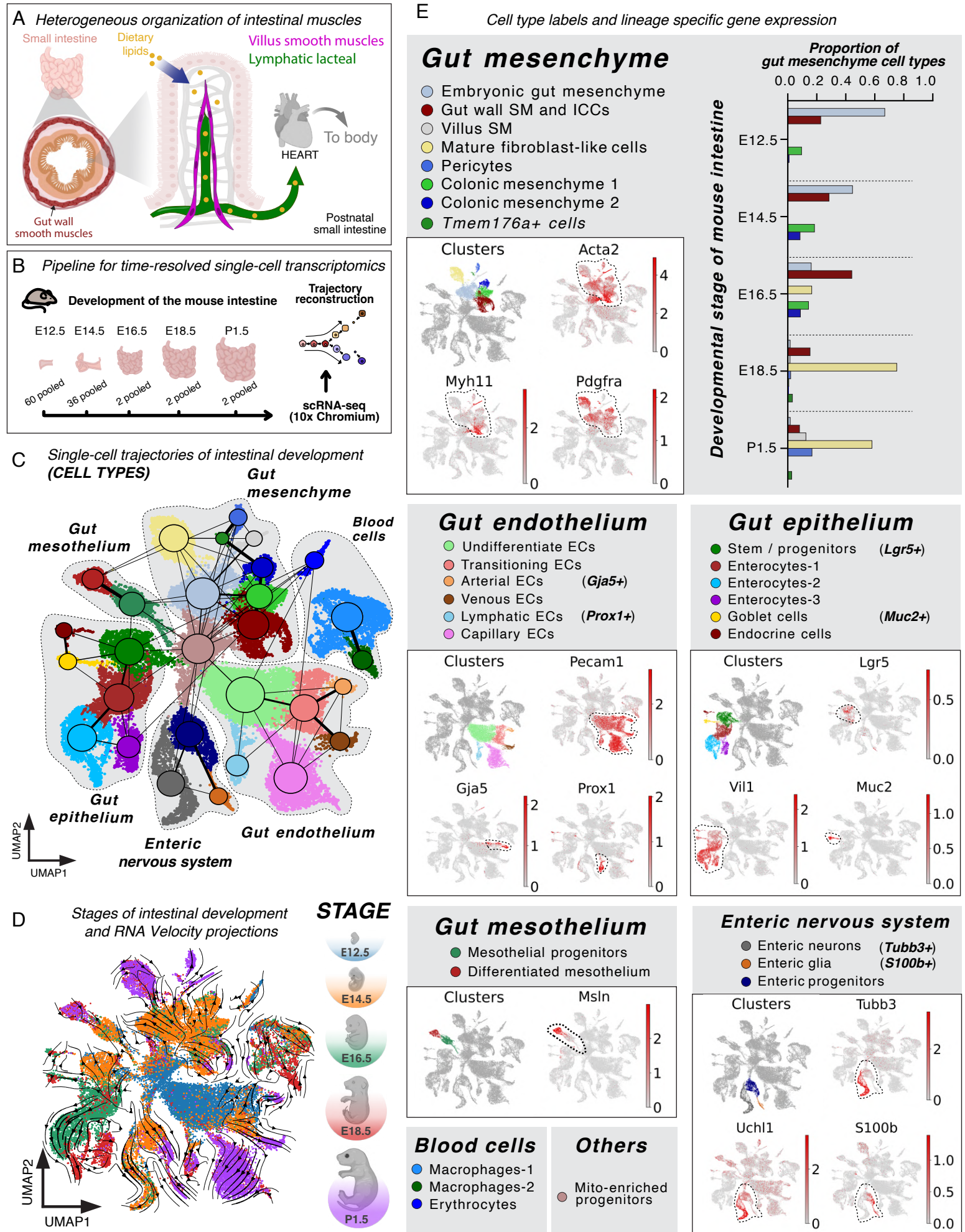
Fig. 1

Figure 2: Reconstructing the developmental trajectories and transcriptional signatures of intestinal musculature. (A) UMAP plot of 7,519 single-cell transcriptomes from the developing small intestinal musculature at E12.5, E14.5, E16.5, and E18.5 and P1.5, clustered by gene expression and colored by cell type labels. The cartoon highlights the relative regions of assembly of the *muscularis externa* and the *muscularis mucosa* within the developing small intestine. PAGA map overlaid on UMAP with circles representing cell types and edges representing global relationships between cell types. **(B)** Boxes colored by cell type labels and UMAP plots showing the expression of selected gene markers (in bold) in the gut musculature scRNA-seq data. **(C)** UMAP plots showing mouse development stages for the small intestinal musculature scRNA-seq data. **(D)** Dendrogram showing hierarchical clustering of mesenchymal cell types in developing gut musculature. **(E)** Immunofluorescent staining of tissue sections for FOXP2 (nuclear) and SMA (cytoplasmic). FOXP2 expression colocalizes with nuclei of gut wall muscles but not SM in the proximal midgut (E14.5) and jejunum (E18.5). **(F)** Immunofluorescent staining of tissue sections for PDGFRα (on cell membrane) and SMA (cytoplasmic). PDGFRα expression was observed in the mesenchymal cells between the endoderm and inner SMA+ SM layer in the proximal midgut at E14.5 and jejunal villus subepithelial mesenchyme at P9. PDGFRα was not expressed in SMA^{high} villus SM at P9. e - endoderm, m - gut tube mesenchyme, gw - gut wall, asterisk (*) - star cell, arrow - spindle-shaped villus SM cell, VSMs - vascular SMs. **(G)** Induction of lineage tracing in *Pdgfra+* cells of pregnant mouse dams at E16.5 results in tdTomato reporter (intracellular) labeling of SMA^{low} star cells (yellow asterisks) in the villus of the mouse pup at E18.5. The yellow box shows a magnified inset of a tdTomato+ SMA^{low} star cell. R26R - Rosa26 reporter. All scale bars = 50μm.
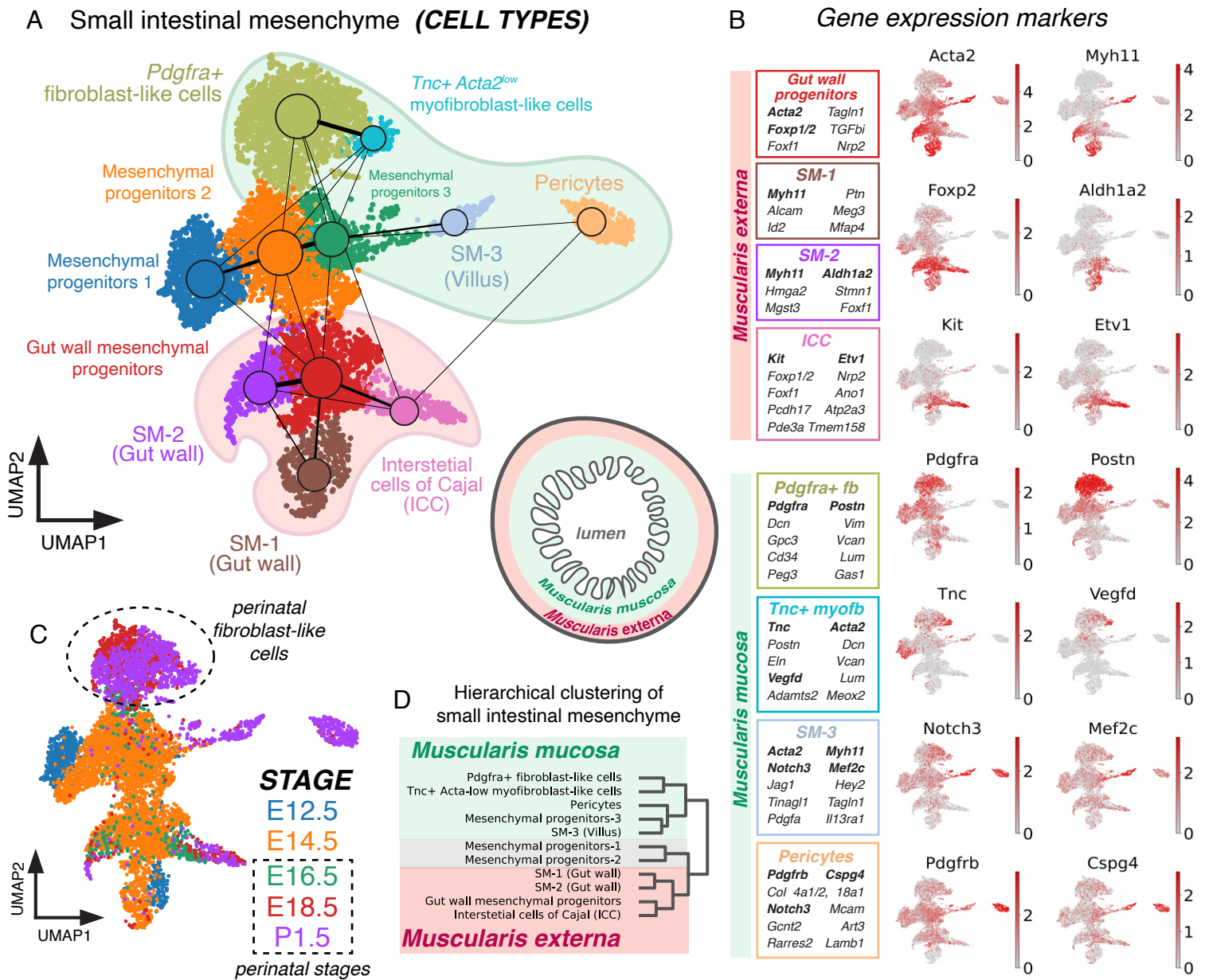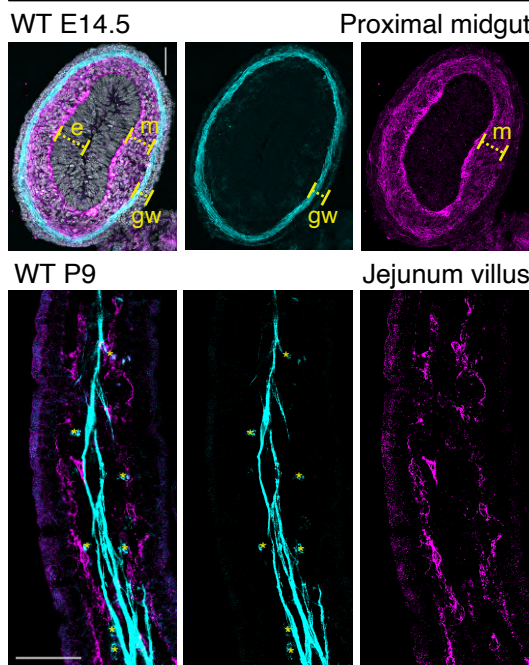
Fig. 2

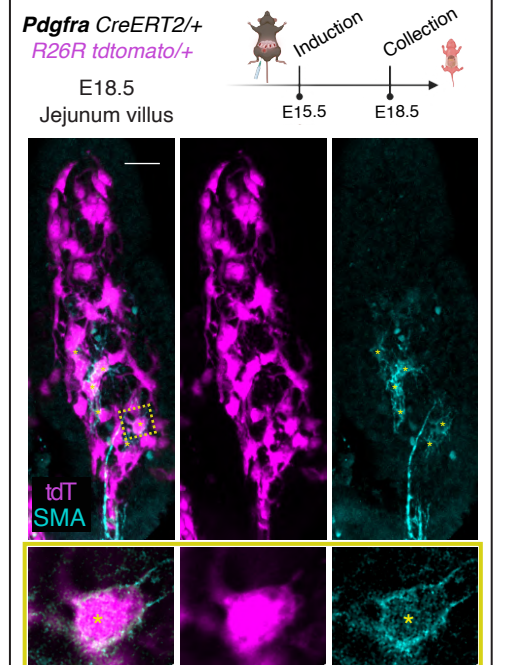**A** Small intestinal mesenchyme *(CELL TYPES)*
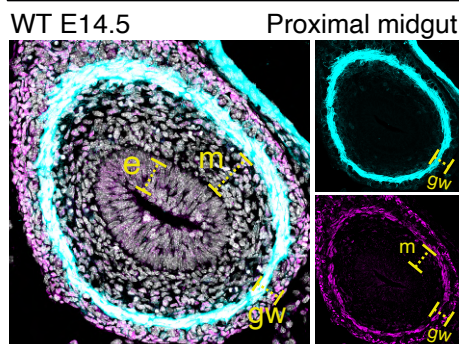
B *Gene expression markers*

Figure 3: Pdgfra+ villus fibroblast-like cells undergo a Tnc+ myofibroblast-like transition to form villus SMs. (A) Schematic for *Pdgfra+* and *Tnc+* lineage tracing in 3 induction-collection intervals of P0i-P9c, P9i-P18c, and P18i-P27c. **(B)** *Pdgfra+* lineage tracing in induction-collection intervals P0i-P9c and P9i-P18c; wholemount immunostaining of SMA on jejunal villi. Boxes (orange and blue) show the region magnified in the inset with a single 1μm section along the whole-mount z stack. Yellow arrows point to SMA+ fibers with tdTomato expression. **(C)** *Pdgfra+* lineage tracing contributions to SM fibers in induction-collection intervals P0i-P9c, P9i-P18c, and P18i-P27c. Comparisons by one-way ANOVA followed by Tukey's multiple comparisons test (presented as mean ± SEM). **(D)** Scatter plots showing co-expression of *Tnc* with *Pdgfra*, *Acta2* and *Myh11* in the cell types of the developing *muscularis mucosa*. **(E)** Immunofluorescent staining of TNC and SMA on jejunal villi at E18.5 and P9. TNC expression (intra/extra cellular) colocalizes with the SMA^{low} star cells but not the SMA^{high} villus SMs. Yellow boxes show the region magnified in the inset. In the P9 insets, yellow asterisks (*) mark SMA+ TNC+ star cells whereas the yellow arrow marks a spindle-shaped SM cell. **(F)** *Tnc+* lineage tracing in induction-collection intervals P0i-P9c and P9i-P18c; wholemount immunostaining of SMA on jejunal villi. Boxes (orange and blue) show the region magnified in the inset with a single 1μm section along the whole-mount z stack. Yellow arrows point to SMA+ fibers with tdTomato expression. **(G)** *Tnc+* lineage tracing contributions to SM fibers in induction-collection intervals P0i-P9c, P9i-P18c, and P18i-P27c. Comparisons by one-way ANOVA followed by Tukey's multiple comparisons test (presented as mean ± SEM). **(H)** Proposed model for myofibroblast-like transition of villus fibroblasts to generate and renew SM in the small intestine. Transitionary cells fall along the continuum of gene expression of SMA (*Acta2*), MYH11, PDGFRα, and TNC. R26R - Rosa26 reporter. All scale bars = 50μm.
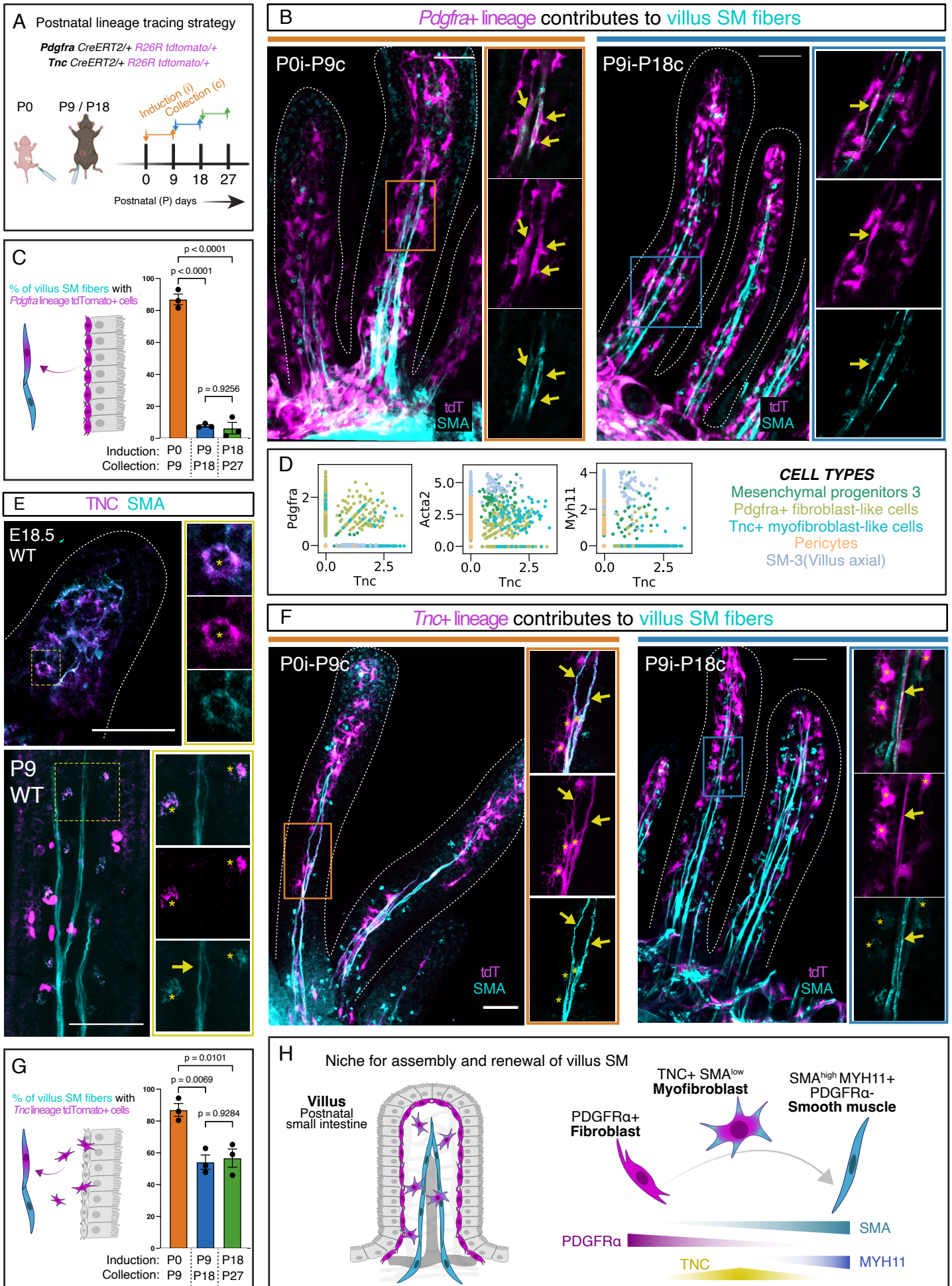
Fig. 3

A Postnatal lineage tracing strategy

Pdgfra CreERT2/+ *R26R tdtomato/+*
Tnc CreERT2/+ *R26R tdtomato/+*

B *Pdgfra+* lineage contributes to villus SM fibers

C % of villus SM fibers with *Pdgfra* lineage tdTomato+ cells

D

CELL TYPES
- Mesenchymal progenitors 3
- Pdgfra+ fibroblast-like cells
- Tnc+ myofibroblast-like cells
- Pericytes
- SM-3(Villus axial)

E TNC SMA

F *Tnc+* lineage contributes to villus SM fibers

G % of villus SM fibers with *Tnc* lineage tdTomato+ cells

H Niche for assembly and renewal of villus SM

Figure 4: **Loss of NOTCH3-DLL4 signaling perturbs villus SM assembly along the lymphatic lacteal. (A)** UMAP plots showing the expression of Notch signaling regulators and effectors upregulated in the villus SM. **(B)** Scatter plots showing co-expression of *Notch3* with SM markers Acta2 and Myh11 in the cell types of the developing *muscularis mucosa*. **(C)** Immunofluorescent staining of jejunal villi tissue sections at E18.5 and P9 for NOTCH3 and SMA. NOTCH3 expression (on cell membrane) colocalizes with the SMA^{low} star cells and SMA^{high} villus SMs (SMA - cytoplasmic). Yellow boxes show the region magnified in the inset. **(D)** Immunofluorescent staining of jejunal villi tissue sections at E18.5 for DLL4 (on cell membrane) and LYVE1 (on cell membrane). The Cyan arrow shows the colocalization of DLL4 and LYVE1 in the lacteal tip cell. **(E)** Representative *Notch3* loss phenotype showing loss of villus SM length and filopodia. **(F)** Wholemount immunofluorescence of SMA and lymphatic marker LYVE1 on villi from the proximal jejunum upon inducing knockout of *Notch3* gene using the *Pdgfra CreERT2* driver (top panel) and *Dll4* gene knockout using *Prox1 CreERT2* (bottom panel). **(G)** Binned quantification of the percentage of villi with given ratios of lacteal and villus SM lengths upon *Notch3* gene knockout using *Pdgfra CreERT2* and *Dll4* iKO using *Prox1 CreERT2*. Compared using two-way ANOVA followed by Šídák's multiple comparisons test (presented as mean ± SEM). **(H)** Proposed model of NOTCH3-DLL4 function in the postnatal structural assembly of the muscular-lacteal complex, as seen at P9. iKO - inducibly knocked out. All scale bars = 50μm.

Fig. 4